ENERGY CONFINEMENT IN ALCATOR

A.Gondhalekar, D.Overskei, R.Parker and J.West

PFC/RR-78-15   December 1978

Francis Bitter National Magnet Laboratory and

Plasma Fusion Center,

Massachusetts Institute of Technology,

Cambridge, Massachusetts 02139

ENERGY CONFINEMENT IN ALCATOR

A.Gondhalekar, D.Overskei, R.Parker and J.West

Francis Bitter National Magnet Laboratory and Plasma Fusion Center
Massachusetts Institute of Technology, Cambridge, MA.02139.

ABSTRACT

Stable discharges with peak density $\hat{n}_e = 1.5 \times 10^{15} \text{cm}^{-3}$ have been obtained in deuterium at $B_T = 8.7T$ in the Alcator tokamak. Complete thermal equilibration between electrons and ions is observed, with peak temperatures of 900eV. The maximum value of $\hat{n}\tau_E$ is $3 \times 10^{13} \text{cm}^{-3}.\text{s}$.

Nearly classical behaviour, from the viewpoint of energy confinement, is observed. At the highest densities, a regime is attained where the anomalous electron thermal conductivity observed at lower densities is suppressed, and the dominant role in energy confinement can be attributed to neoclassical ion thermal conduction. The anomalous electron thermal conduction varies inversely with density. The observed ion thermal conductivity is neoclassical at high density, but seems to be somewhat greater at density less than $2 \times 10^{14} \text{cm}^{-3}$.

Dependence of energy confinement on B_T is also investigated. With constant $\bar{n}_e$ and I_p, no significant effect of increasing B_T on τ_E is observed. However, the highest achievable density and τ_E increase with B_T.

Stable operation of high current, low q_L discharges has been achieved. Energy confinement for such discharges is described. Some improvement in τ_E is observed at high current.

I INTRODUCTION

An essential advance in experimental tokamak physics in recent years has been in the ability to obtain high density plasmas with moderate temperatures. The plasma density now attainable is 10-100 times larger than that possible only a few years ago. Operation at higher densities has been accompanied by substantial improvement in energy confinement. The high density regime first observed in Alcator has since been attained in many other tokamaks. Although it is not yet clear what factors favour the ability to obtain high density, available heating power would seem to be one of the more important ones. Tokamaks with low impurity content and high toroidal magnetic field and hence high ohmic heating power density have, therefore, yielded the highest density and relatively high values for energy confinement. In Alcator, the maximum peak density, $\hat{n}_e$, so far achieved is $1.5 \times 10^{15} cm^{-3}$ with an energy confinement time τ_E = 20ms., giving $\hat{n}\tau_E = 3 \times 10^{13} cm^{-3}.s$ at peak electron and ion temperatures of 900eV.

A description of the Alcator tokamak has been given elsewhere[1]. It is a device with major radius R=54cm and limiter radius a_L=10cm. The unique capability of Alcator to operate over a wide range of parameters, with toroidal field 3T $\leqslant B_T \leqslant$ 9T, plasma current 80kA $\leqslant I_p \leqslant$ 300kA, and line averaged density $5 \times 10^{12} cm^{-3} \leqslant \bar{n}_e \leqslant 7.5 \times 10^{14} cm^{-3}$, has enabled study of the dependence of energy confinement on these parameters. The advantages of high density operation have been discussed previously[2,3]. In this paper, further elucidation of this behaviour is given. We show that the higher density discharges can be understood as determined by neoclassical ion thermal conduction in the central core, whereas at lower densities anomalous electron thermal conduction dominates. A preliminary account of these observations has been given earlier[4,5,6].

High density discharges are obtained by neutral gas injection into the plasma. Equilibrium is first established in a low density plasma with $\bar{n}_e \simeq 3 \times 10^{13} cm^{-3}$. Neutral gas is then injected at the edge of the plasma through a programmable fast valve, bringing the density to the desired value[3]. Energy confinement studies discussed here were

performed under stationary discharge conditions. Much effort was invested in 'tuning' the machine to give optimum performance. This roughly entails adjusting the various equilibrium fields and the temporal behaviour of density and plasma current until the lowest plasma resistance is observed for the required values of B_T, I_p and $\bar{n}_e$. Thus radiative power loss due to impurities is minimised for the data reported here. In section III the dependence of energy confinement on density is described. A brief description of the influence of toroidal magnetic field and plasma current on energy confinement is given in sections IV and V. Other aspects of high current, low q_L discharges have been discussed elsewhere[7].

II PLASMA REGIMES

Fig.1 illustrates one of the highest density discharges obtained with $\bar{n}_e = 7.2 \times 10^{14} cm^{-3}$. Peak density $\hat{n}_e = 1.5 \times 10^{15} cm^{-3}$, and peak temperatures $T_{e,i} = 900eV$ were observed. Loop voltage V_R, plasma current I_p and density $\bar{n}_e$ were maintained constant within 10% for 100ms. Peak density of greater than $10^{15} cm^{-3}$ was maintained for about 150ms.

The experiments described in the remainder of this paper were carried out in deuterium with $B_T = 6T$, $130kA \leqslant I_p \leqslant 160kA$ and $5 \times 10^{13} cm^{-3} \leqslant \bar{n}_e \leqslant 6 \times 10^{14} cm^{-3}$. Fig.2 shows typical radial profiles of electron temperature, $T_e(r)$, and electron density, $n_e(r)$, measured by Thomson scattering of ruby laser radiation. The electron temperature profile is best described by

$$T_e(r) = \hat{T}_e \exp(-r^2/a_T^2)$$

The radial profiles of current density, $j(r)$, and safety factor, $q(r)$, are determined in the usual way by assuming $j(r) \propto T_e^{3/2}(r)$. Clean vacuum and wall conditions in Alcator permit plasmas to be produced whose resistivity is nearly equal to the calculated classical value. Thus the effective ion charge in the plasma, Z_{eff}, is close to unity.

For discharges studied here, we find that the safety factor on axis, q_o, always assumes a minimum value, $0.85 \leqslant q_o \leqslant 1$. This is in

agreement with deductions made from sawtooth X-ray emission signals[8]. With the profile given above and $Z_{eff}(r) \simeq 1$, it is easily shown that $a_T^2 q_L \simeq \frac{3}{2} r_C^2 q_o$. r_C is the radius of the current channel which can be smaller than a_L due to displacement of the plasma column; usually $9.5cm \lesssim r_C \lesssim a_L = 10cm$. q_L is the safety factor at the limiter. Empirically, $a_T^2 q_L \simeq 120$ cm^2 is measured in Alcator.

Furthermore, assuming that the induced toroidal electric field is constant across the plasma cross-section, $E(r) = constant = V_R/2\pi R$, it is easily shown, with Spitzer-Härm resistivity, that for a deuterium plasma

$$\hat{T}_e \simeq 4 \times 10^2 (B_T \cdot Z_{eff}/V_R \cdot q_o)^{2/3} eV$$

B_T is in tesla and the the loop-voltage V_R is in Volts. Measurements of electron temperature under a large variety of plasma conditions bear out these relationships with $Z_{eff} \simeq 1$ and $0.85 \lesssim q_o \lesssim 1$. This confirms, albeit only for clean plasmas, an early intuition[9] that to know the temperature and its distribution in an ohmically heated tokamak plasma, one need measure only the loop voltage, plasma current and toroidal magnetic field.

The density profile is best described by

$$n_e(r) = \hat{n}_e \left\{ 1 - r^2/a_L^2 \right\}^\alpha$$

The value of α depends on the density. For experiments considered here, with $B_T = 6T$, $I_P \simeq 150kA$, the value of α increases approximately linearly from 0.75 at $\bar{n}_e \simeq 10^{14} cm^{-3}$ to 2.0 at $\bar{n}_e = 6 \times 10^{14} cm^{-3}$. No simple relationship between α and $\bar{n}_e$ could be established as in the case of q_L (or I_P/B_T) and a_T^2 above. The value of α will depend in a complicated way on the mechanism of gas ingestion at the plasma edge, and transport of plasma to the center of the discharge, processes which are not understood at present. During gas injection, the electron density evolves without significant inversion, $(dn_e/dr \geq 0)$, in the radial profile[2]. This would seem to exclude certain models of plasma density build-up in which transport of plasma to the center of the column is sustained by instability induced by unfavourable gradients of plasma

density.

It has been postulated that the neoclassical pinch might operate in Alcator to transport plasma formed at the edge of the column to the center against the density gradient[10]. The neoclassical pinch effect is strong only when $\nu_{*e} < 8$. Near the edge, ν_{*e} is large and the pinch effect is correspondingly weak. However, the small density inversion observed at the edge[2] may cause rapid transport across the edge region $7cm \leqslant r \leqslant 10cm$. At $r < 7cm$, the pinch effect will efficiently convect plasma to the interior. Fig.3 shows the radial variation of ν_{*e} for low and high density discharges. As density increases and the plasma becomes more collisional, the pinch effect weakens and eventually stops. This could be the origin of the 'density limit' observed experimentally. In Alcator, at given B_T and I_p, density can be increased until ν_{*e} (minimum) $\simeq$ 8-10. Attempts to increase the density further by injection of additional neutral gas at the edge cause disruption. The density can be increased by raising B_T and I_p. This has the effect of increasing the temperature and reducing ν_{*e}. Density can then be increased until again ν_{*e} (minimum) $\simeq$ 8-10. In discharges where $\bar{n}_e$ is maintained at a constant value, the ratio $\hat{n}_e / \bar{n}_e$, and hence the value of α, are observed to increase continuously, indicating steady convection of plasma to the center. All these observations can be accounted for in a semi-quantitative way by model computations using the neoclassical pinch[10].

Measurements of peak ion temperature are made by analysis of charge-exchanged neutral particles emitted from the plasma, and for discharges in deuterium, also by using the thermonuclear neutron yield[3,11]. Ion temperatures so determined are consistent with

$$\hat{P}_{OH} = E \cdot j_o \simeq \frac{3}{2} \hat{n}_i (\hat{T}_e - \hat{T}_i)/\hat{\tau}_{ei}$$

$\hat{\tau}_{ei}$ is the electron-ion equilibration time at plasma center, $\hat{P}_{OH}$ is the peak ohmic power input. This relation gives the maximum temperature difference that can be sustained by the available heating power.

Measurements indicate peak ion temperatures typically only about 100eV less than the corresponding electron temperature at high density. The variation of peak electron and ion temperatures with density is shown in Fig.4[11].In the following, the ion temperature profile is assumed to be of the same shape as the electron temperature profile.

A rough characterization of the plasma regimes realized in Alcator under these conditions can be obtained from the values of various dimensionless parameters: the collisionality parameter for trapped particles, $\nu_* = 2^{1/2}\nu(qR/V_{th})(R/r)^{3/2}$, the collisionality parameter for transit particles, $\nu_{**} = \nu(qR/V_{th})$, the streaming parameter, $\langle \xi \rangle = \langle v_{drift}/v_{thermal} \rangle$, and the ratio of the applied electric field to the critical run-away field, $\langle E/E_{CR} \rangle$. Fig.3 shows the radial variation of ν_* , ν_{**}, and the safety factor q. The plasma can be characterized as being predominantly in the plateau regime of neoclassical theory, verging on the Pfirsch-Schlüter regime.

III DENSITY DEPENDENCE OF ENERGY CONFINEMENT

A study of the variation of energy confinement and power balance with density, at constant toroidal magnetic field B_T =6T, and plasma current, $130kA \lesssim I_P \lesssim 160kA$, has been made in order to ascertain how closely energy confinement approaches neoclassical values. The global energy confinement time is defined as

$$\tau_E(EX) = 2\pi R \int_0^{a_L} \frac{3}{2}(n_i T_i + n_e T_e)2\pi r\,dr / I_P V_R$$

V_R is the resistive part of the loop-voltage induced around the torus. V_R is determined from the measured total loop-voltage V_L, corrected for the time variation of poloidal flux between the plasma and the voltage loops, where the mutual inductance involved has been measured directly.

Fig.5 illustrates the variation of the induced voltage with density, showing a gradual increase in V_R, corresponding to steadily falling electron temperature as density increases. This may be understood as due to increased power transfer to the ions and their steadily growing role in energy loss. The variation with density of the

experimentally determined energy confinement time τ_E (EX) is shown in Fig.6. We observe that τ_E (EX) increases approximately linearly with $\bar{n}_e$ at constant B_T and I_P. The curve labelled τ_E (NC) in Fig.6 gives the value of the energy confinement time if neoclassical ion thermal conduction were the dominant energy loss mechanism, for plasma conditions identical to those in the experiment. The neoclassical energy confinement time at each point, τ_E^{NC} (r), is calculated from

$$\tau_E^{NC}(r) = \frac{\int_0^r 2\pi r'\left\{\frac{3}{2}(n_iT_i + n_eT_e)\right\}dr'}{2\pi r Q_i^{NC}(r)}$$

$Q_i^{NC}(r)$ is the heat flux due to neoclassical ion thermal conduction. τ_E (NC) is then the value of $\tau_E^{NC}(r)$, line averaged over a region $0 \leqslant r \leqslant 0.7a_L$. Neoclassical coefficients given by Hazeltine and Hinton[12] are used in these computations. Energy confinement time within a factor of 1.4 of the neoclassical value is observed at the highest density. Comparison between the two curves shows that the plasma is afflicted with anomalous energy loss at low density, and that this loss is reduced as density increases in Alcator. This excess energy loss is attributed to anomalous radial electron heat conduction. We show later that the anomalous electron heat conductivity is suppressed as density increases.

Fig.7 shows the variation of poloidal-beta, β_P, with density $\bar{n}_e$. β_P is defined as

$$\beta_P = 8\pi < n_iT_i + n_eT_e > /B_P^2$$

β_P is the ratio of the plasma kinetic pressure and the pressure of the poloidal magnetic field B_P. The maximum value of β_P is also in accord with neoclassical estimates.

The linear dependence of the energy confinement time on $\bar{n}_e$ is not a unique way of representing the variation of τ_E. Fig.8 shows the dependence of τ_E on the streaming parameter $< \xi >$. Strong correlation between the two may be deduced. Wobig[13] has shown that this

representation may be more generally applicable when comparing different tokamaks with each other, or with stellarators. Energy confinement properties of stellarators have thus been attributed to relatively low current density in these devices[13].

Fig.9 shows the same data, indicating the dependence of τ_E on the collisionality parameter for trapped electrons, $\langle \nu_{*e} \rangle$, averaged over $0 \leqslant r \leqslant 0.6a_L$. Again, strong correlation between τ_E and $\langle \nu_{*e} \rangle$ may be deduced.

Each of these dependences implies a different mechanism for energy loss. It should be emphasised that it is not possible to vary $\bar{n}_e$, $\langle \xi \rangle$ or $\langle \nu_{*e} \rangle$ independently of the other two, and therefore it is not possible to choose between the many possiblities. There are several theories that purport to be able to explain these observations. However, the data is not accurate or complete enough, nor are the theories definite enough in their forecasts to be falsifiable with the aid of available data.

Radial electron heat conduction has long been identified as the major anomalous energy loss mechanism in tokamaks[14]. It has also been known that small perturbations of the confining magnetic field cause the rapid electron heat conduction along such a field to thermally connect the interior of the plasma column to an exterior wall or limiter[15,16,17]. Such situations are familiar in the literature on astrophysical plasmas[18]. The subject of anomalous heat conduction in a tokamak has recently received renewed and more sophisticated treatment[19,30].Experimental verification of magnetic field fluctuations as the cause of anomalous radial heat conduction in Alcator has also been claimed[20].

Power balance in the central core of the plasma is next examined. Energy confinement time at the plasma center, τ_{Eo}, is defined as

$$\tau_{Eo} = \frac{3}{2} (\hat{n}_i \hat{T}_i + \hat{n}_e \hat{T}_e)/E \cdot j_o$$

Here, the peak densities $\hat{n}_{e,i}$, peak electron and ion temperatures $\hat{T}_e$ and $\hat{T}_i$, are directly determined. The peak current density, j_o, is deduced

from $\hat{T}_e$ by assuming Spitzer-Härm resistivity and that the induced toroidal electric field E is uniform across the plasma cross-section. The value of j_0 is consistent with the current distribution deduced from the electron temperature profile. It is also in agreement with $0.85 \leqslant g_0 \leqslant 1$. Fig.10 shows the variation of τ_{Eo} with the peak density, at constant B_T and I_p. τ_{Eo} does not increase linearly with density but seems to saturate. This variation of τ_{Eo} at high density, akin to the neoclassical, indicates that the core of the plasma column may be dominated by neoclassical losses.

Since, at high density, most of the energy transport out of the core seems to be attributable to ion heat conduction, the ohmic heat input may be put equal to the neoclassical ion conduction loss and the ion temperature and its distribution computed and compared to the experimental value. We thus have

$$Q_{OH}(r) = P_{OH}/2\pi r = \int_0^r 2\pi r' E \cdot j(r')dr'/2\pi r$$

We then put, for $r \leqslant 5cm$

$$\delta Q_i^{NC}(r) = Q_{OH}(r)$$

Two model ion temperature profiles were substituted into the expression for $Q_i^{NC}(r)$. They were of the form

$$T_i(r) = \Sigma a_n r^{2n}, \quad n=0,1,2,3$$

and

$$T_i(r) = a_1 \exp(-a_2 r^2)$$

Both models give the same peak temperature, which is in agreement with the measured value[3,11]. Fig.11 shows the result of the calculation using the gaussian model. The effects of possible departures of the ion thermal conductivity from neoclassical are also included. The upper dotted curve in Fig.11 shows the result with an anomaly factor, δ, of unity(ion thermal conduction equal to the neoclassical). The error-bar

at the peak indicates the uncertainity in the calculation. We see that within the accuracy of the calculation, the experimental peak ion temperature can be accounted for by an ion thermal conductivity equal to the neoclassical. In the lower dotted curve in Fig.11, an anomaly factor of 1.5 is employed; i.e. the neoclassical ion heat flux is multiplied by a factor of 1.5 everywhere. The deduced peak ion temperature is then well short of the measured, implying that for these plasma conditions an anomaly, if any, in the ion thermal conductivity is less than 1.5 of neoclassical. This agreement confirms the correctness of attributing the dominant role in energy loss, at high density, to neoclassical ion thermal conduction. As expected, gross disagreement with measurement is obtained when the above procedure is applied to low density discharges, as shown in Fig.12, demonstrating the existence, at low density, of a dominant energy loss process other than neoclassical ion thermal conduction.

Radial fluxes for $r \leqslant 0.5a_L$ may be deduced from the experimental values of $n_e(r)$, $T_e(r)$ and $T_i(r)$, neglecting losses due to radiation and charge-exchange. At plasma densities $\bar{n}_e \geqslant 2 \times 10^{14}$ cm^{-3}, the central core of the plasma is opaque to neutral particles of energy less than 1keV. Charge-exchange losses for such plasmas are important only for the region r>5cm. Spatially and temporally resolved bolometric measurements of radiative and charge-exchange losses[21] show that for plasma and machine conditions involved in the studies reported here, neglecting these losses does not significantly affect calculation of power balance in the central core of the plasma, defined as the region $0 \leqslant r \leqslant 5$cm.

The equilibration power transferred from the electrons to the ions, $P_{ei}(r)$, is set equal to the power transported by the ions, $P_i(r)$,

$$P_i(r) = P_{ei}(r) = \int_0^r 2\pi r' [\frac{3}{2} n_i (T_e - T_i)/\tau_{ei}] dr'$$

τ_{ei} is the electron-ion equilibration time[22]. The ion heat flux is then

$$Q_i^{EX}(r) = P_i(r)/2\pi r$$

The ion thermal diffusivity $\chi_i^{EX}(r)$, is determined from

$$Q_i^{EX}(r) = -\chi_i^{EX}(r) \cdot n_i(r) \cdot \nabla T_i(r)$$

The power transported by the electrons, $P_e(r)$, is then given by

$$P_e(r) = P_{OH}(r) - P_{ei}(r) = \int_o^r 2\pi r' E \cdot j(r')\, dr' - P_{ei}(r)$$

The electron heat flux, $Q_e^{EX}(r)$, and the electron thermal diffusivity $\chi_e^{EX}(r)$ are determined as for the ions. At $\bar{n}_e > 3 \times 10^{14} cm^{-3}$, the experimental determination of P_{ei} is uncertain owing to the small difference between electron and ion temperatures. This gives rise to uncertainties in the calculated heat fluxes at high density. Fig.13 shows the ratios of the experimentally determined electron heat flux and the neoclassical electron heat flux at $\bar{n}_e = 1.4 \times 10^{14} cm^{-3}$ and $\bar{n}_e = 5.5 \times 10^{14} cm^{-3}$.

We observe that at low density, the electron heat flux is 200 times larger than the neoclassical, as seen in other tokamaks[23]. When radiative and charge-exchange losses are properly included, this factor of 200 might be reduced to 100-150. As density increases in Alcator, this anomaly in the electron heat flux diminishes, until at $\bar{n}_e > 5 \times 10^{14} cm^{-3}$ it is at most ten times larger than the neoclassical loss by the electrons. Lastly, knowing the ion and electron heat fluxes, $Q_i^{EX}(r)$ and $Q_e^{EX}(r)$ respectively, the ion and electron heat diffusivities may be computed and compared to the neoclassical values. Fig.14 shows the variation of χ_i^{EX} and χ_e^{EX}, averaged over $3cm \leqslant r \leqslant 5cm$, with density $\bar{n}_e$. The corresponding neoclassical heat diffusivities, χ_i^{NC} and χ_e^{NC}, are also shown. We see that $\chi_e^{EX} \propto 1/\bar{n}_e$ and again that at $\bar{n}_e = 5.5 \times 10^{14} cm^{-3}$, $\chi_e^{EX} \leqslant 10\,\chi_e^{NC}$ whereas at $\bar{n}_e = 10^{14}\ cm$, $\chi_e^{EX} \gg \chi_e^{NC}$. For the ions, $\chi_i^{EX} \simeq \chi_i^{NC}$ for $\bar{n}_e \geqslant 3 \times 10^{14} cm^{-3}$, but shows an unfavourable trend at $\bar{n}_e \leqslant 2 \times 10^{14}\ cm^{-3}$ where $\chi_i^{EX} \simeq 1\text{-}2\,\chi_i^{NC}$, as previously suspected in the TFR tokamak[24]. We conclude from this study that as density is increased in Alcator, a gradual transition from the anomalous electron thermal conduction regime to the neoclassical ion thermal conduction regime takes place in the central core of the plasma.

IV TOROIDAL MAGNETIC FIELD DEPENDENCE OF ENERGY CONFINEMENT

The dependence of τ_E on B_T has been investigated by keeping $\bar{n}_e$ and I_p constant and varying B_T. Experiments were conducted with B_T =3.5T and B_T =7.7T in deuterium at $\bar{n}_e \simeq 2 \times 10^{14} cm^{-3}$ and I_p =115kA. No obvious differences were observed in the macroscopic properties of the plasma, such as Z_{eff} or MHD activity. Both discharges showed similar temporal characteristics, with small sawtooth fluctuations on X-ray emission. Measured profiles of electron density and temperature are shown in Fig.15. The density profiles in both cases are similar. However, the peak electron temperature, $\hat{T}_e$, increases and the temperature profile narrows when B is increased. This is in accordance with $\hat{T}_e \alpha (B_T/V_R)^{2/3}$ and $a_T^2 \alpha I_p/B_T$ as discussed earlier. The ion temperature also shows similar dependence on B_T [11]. The total energy content is nearly the same for the two discharges, and since the power input is also nearly equal, the energy confinement time, $\tau_E \simeq 9ms$, remains unchanged when B_T is increased.

Fig.16 shows more data along these lines. The plasma conditions were not as uniform as in the example just given. The data reenforces the observation that at fixed density the energy confinement is not affected by the toroidal magnetic field, as shown by the dotted lines. However, the highest density, and therefore the maximum attainable energy confinement, increase with B_T, as shown by the solid line in Fig.16. This seems to be the chief merit of an ohmically heated high field tokamak. The physical understanding of this result is as follows: At constant density and plasma current, increasing B_T has an insignificant effect on τ_E because although the peak energy density increases with B_T, the temperature profile narrows so that the average energy density remains the same as that at lower B_T. With larger B_T, the facility for higher plasma current density and consequently ohmic input power density increases. This permits higher plasma density to be obtained. Since energy confinement improves with density, the maximum achievable energy confinement time also increases with B_T.

V   PLASMA CURRENT DEPENDENCE OF ENERGY CONFINEMENT

For the successful operation of a self-sustaining controlled fusion device, it is essential to efficiently confine and equilibrate the high energy charged particle products of a fusion reaction. This is a means of "boot-strap" heating of the plasma. This requirement for efficient confinement of high energy charged particles applies also to all the auxiliary plasma heating methods in use at present. In a tokamak, the confinement of high energy charged particles is achieved with the aid of the poloidal magnetic field. Thus, it is important to be able to operate a tokamak with the largest possible plasma current compatible with MHD stability and favourable energy confinement. In the past, these requirements have been thought to be incompatible. Large currents made the plasma more susceptible to severe MHD activity which in turn degraded energy confinement[25,26]. In keeping with this thinking, energy confinement was belived to depend on $(B_T/I_p)^{1/2}$ in Alcator[2]. We have sought to reexamine this dependence with more accurate and complete diagnostics, and technical improvements which permit us a larger latitude in available density, plasma current and of course the toroidal field. The dependence of τ_E on B_T was discussed in the previous section. Here, we present studies of the behaviour of τ_E at high plasma current. Stable discharges with $q_L=1.9$ have been obtained, but not enough to study systematically. The high current, low q discharges investigated were in deuterium, with $B_T=6T$, $2\times10^{14} cm^{-3} \leqslant \bar{n}_e \leqslant 5\times10^{14} cm^{-3}$, $215kA \leqslant I_p \leqslant 235kA$ and $2.4 \leqslant q_L \leqslant 2.6$. At constant B_T the temperature profile is much wider for the high current discharges than for the lower current ones, again according to $a_T \propto I_p/B_T$. The peak electron temperature rises by about 15%. The peak ion temperature shows a similar increase[11]. The measured energy confinement times at various densities are shown in Fig.17(solid points). For comparison, confinement times for the same $\bar{n}_e$ and B_T but lower plasma current, $130kA \leqslant I_p \leqslant 160kA$, are shown (dotted line $\tau_E(EX)$). We observe that in all cases the confinement time is at least as good as, if not somewhat greater than, that at lower current. It must be remarked that it is

more difficult to obtain stable high current discharges than low current ones with $q_L \geqslant 3$. At present, the probability of producing a stable high current discharge is smaller than that for a low current one. But it seems to be only a matter of gaining more understanding of the necessary machine 'tuning' in order for reliable high current operation to become routine. High current discharges that do survive show no degradation of energy confinement; indeed some improvement seems possible.

In Fig.17 the corresponding neoclassical energy confinement times, $\tau_E(NC)$, are also shown. It is tempting to infer from the observed improvement in $\tau_E(EX)$ with higher current that all is in accord with the dominant role of neoclassical ion loss. However, such inference seems susceptible to fundamental criticism. With high current the gap between $\tau_E(NC)$ and the measured confinement time widens. The electron thermal diffusivity χ_e^{EX} also shows an increase in the high current case over the corresponding value for low current discharges. This may correspond to the reported dependence of anomalous electron thermal conductivity on the temperature profile, i.e. χ_e^{EX} for discharges with flat profiles appears to be greater than that for cases with peaked profiles[27]. Furthermore, the absence of a significant effect of B_T on $\tau_E(EX)$ should also caution us about the role of high current in energy confinement.

Lastly, the important point about high current in a tokamak is that it is beneficial to confinement of high energy charged particles. Observations from RF heating experiments on Alcator[28] allow a tentative conclusion that this expectation is fulfilled.

VI $\quad \hat{n}\tau_E$

In conclusion, since τ_E increases with $\bar{n}_e$, the quality factor, $\hat{n}\tau_E$, increases in proportion to $\bar{n}_e^2$, as shown in Fig.18. The strong dependence of $\hat{n}\tau_E$ on $\bar{n}_e$ facilitates conception of relatively compact high power-density fusion reactors. Detailed tokamak reactor design calculations reveal that the high field, high density tokamak approach offers great promise for rapid progress in the development of fusion

power production[29]. Compact tokamak ignition experiments based on these notions are also under consideration.

ACKNOWLEDGEMENTS

REFERENCES

[1] U.Ascoli-Bartoli, G.Bosia, G.Boxman, P.Brossier, B.Coppi, L.De Kock, B.Meddens, B.Montgomery, A.Oomens, L.Ornstein, R.Parker, L.Pieroni, S.Segre, R.Taylor, P.Van Der Laan and R.Van Heyningen. Proceedings of the Fifth International Conference on Plasma Physics and Controlled Nuclear Fusion Research, Tokyo, Japan, 1974.

[2] E.Apgar, B.Coppi, A.Gondhalekar, H.Helava, D.Komm, F.Martin, B.Montgomery, D.Pappas, R.Parker and D.Overskei. Proceedings of the Sixth International Conference on Plasma Physics and Controlled Nuclear Fusion Research, Berchtesgaden, W.Germany, 1976.

[3] M.Gaudreau, A.Gondhalekar, M.H.Hughes, D.Overskei, D.Pappas, R.R.Parker, S.M.Wolfe, E.Apgar, H.Helava, I.H.Hutchinson, E.S.Marmar and K.Molvig. Phys. Rev. Letters 39(1977)1299.

[4] A.Gondhalekar, D.Overskei, R.R.Parker and J.West. Bull.Am.Phys.Soc., 22(1977)1092.

[5] A.Gondhalekar, R.Granetz, D.Gwinn, I.Hutchinson, B.Kusse, E.Marmar, D.Overskei, D.Pappas, R.R.Parker, M.Pickrell, J.Rice, L.Scaturro, J.Schuss, J..West, S.Wolfe, R.Petrasso, R.E.Slusher and C.M.Surko. Proceedings of the Seventh International Conference on Plasma Physics and Controlled Nuclear Fusion Research, Innsbruck, Austria, August 1978.

[6] A.Gondhalekar, D.Overskei, R.R.Parker and J.West. International Conference on Solids and Plasmas in High Magnetic Fields, Cambridge, U.S.A., September 1978.

[7] D.O.Overskei, A.Gondhalekar, I.Hutchinson, D.Pappas, R.Parker, J.Rice, L.Scaturro, and S.Wolfe. International Conference on Solids and Plasmas in High Magnetic Fields, Cambridge, U.S.A., 1978.

[8] D.Gwinn and R.Granetz. MIT Plasma Fusion Center Report PFC/RR-78-8(1978).

[9] R.Taylor. 1975 Quotation.

[10] M.H.Hughes. Princeton University Plasma Physics Laboratory Report PPPL-1411(1978).

[11] D.S.Pappas and R.R.Parker. MIT Plasma Fusion Center Report
PFC/RR-78-5(1978).

[12] R.D.Hazeltine and F.L.Hinton. Physics of Fluids 16(1973)1883.

[13] H.Wobig, Max-Planck-Institut fur Plasmaphysik, Garching, W.Germany.
Private communication, August 1978.

[14] L.A.Artsimovich. Nuclear Fusion 12(1972)215.

[15] M.G.Rusbridge and P.A.H.Saunders. Report of the Culham Laboratory
Study Group on Plasma Instibilities, CLM-M21, March 1963.

[16] M.G.Rusbridge. Plasma Physics 11(1969)35.

[17] D.H.Birdsall, S.A.Colgate, H.P.Furth, C.W.Hartman and
R.L.Spoerlein. Nuclear Fusion Suppl. Pt.3(1962)955.

[18] J.R.Jokipii. Reviews of Geophysics and Space Physics 9(1971)27.

[19] J.D.Callen. Phys. Rev. Lett. 39(1977)1540.

[20] K.Molvig, J.E.Rice and M.S.Tekula. Phys. Rev. Lett. 41(1978)1240.

[21] L.Scaturro and M.Pickrell. Bull. American Physical Society
23(1978)873.

[22] S.I.Braginskii. In: Reviews of Plasma Physics, M.A.Leontovich, ed.
(Consultants Bureau, New York), 1(1965)205.

[23] EQUIPE TFR. Proceedings of the Sixth International Conference on
Plasma Physics and Controlled Nuclear Fusion Research, Berchtesgaden,
W.Germany, 1976.

[24] EQUIPE TFR. Proceedings of the Seventh International Conference on
Plasma Physics and Controlled Nuclear Fusion Research, Innsbruck,
Austria, August 1978.

[25] S.V.Mirnov and I.B.Semenov. Proceedings of the Fourth International
Conference on Plasma Physics and Controlled Nuclear Fusion Research,
Madison, U.S.A., 1971.

[26] S.V.Mirnov. Paper presented at the IAEA Advisory Group meeting on
Transport Processes in Tokamaks, Kiev, U.S.S.R., November 1977.

[27] B.B.Kadomtsev. Nuclear Fusion 18(1978)553.

[28] J.Schuss and R.R.Parker, Alcator Group. December 1978,
Private Communication.

[29] D.R.Cohn, R.R.Parker and D.L.Jassby. Nuclear Fusion 16(1976)31 and
16(1976)1045.

[30] W.Horton and R.D.Estes. University of Texas Fusion Research Center
Report FRCR 170, May 1978.

FIGURE CAPTIONS

FIG.1 Oscillograph of an ultra-high density discharge in Alcator. Maximum value of $\bar{n}_e$ is $7.2 \times 10^{14} cm^{-3}$. Discharge is in deuterium, with $B_T = 8.7T$ and $I_p = 235kA$. Time: 50ms/div.

Fig.2 Radial profiles of electron temperature and density for two value of $\bar{n}_e$, in deuterium with $B_T = 6T$, $130kA \lessgtr I_p \lessgtr 160kA$.

Fig.3 Radial variation of the collisionality parameters ν_* and ν_{**} for electrons and ions at two values of $\bar{n}_e$. Radial profile of the safety factor, $q(r)$, and values for $< \xi >$ and $<E/E_{CR}>$ are also shown. D_2 plasma, $B_T = 6T$, $130kA \lessgtr I_p \lessgtr 160kA$.

Fig.4 Variation of peak electron and ion temperatures with $\bar{n}_e$, showing nearly complete equilibration at high density.

Fig.5 Variation of the resistive loop-voltage, V_R, with density. D_2 plasma, $B_T = 6T$, $130kA \lessgtr I_p \lessgtr 160kA$.

Fig.6 Variation of the measured energy confinement time $\tau_E(EX)$ with density $\bar{n}_e$. Also shown is the neoclassical energy confinement time $\tau_E(NC)$ for identical plasma conditions. The figure means that if neoclassical ion thermal conduction were the dominant energy loss mechanism, the power needed to sustain these plasmas would be lot less than what is measured.

Fig.7 Variation of poloidal-beta, β_P, with density.

Fig.8 Variation of $\tau_E(EX)$ with the average streaming parameter, $< \xi >=<V_{drift}/V_{thermal}>$.

Fig.9 Variation of $\tau_E(EX)$ with the average collisionality parameter for trapped electrons, $< \nu_{*e}>$.

Fig.10 Energy confinement time τ_{Eo} at plasma center plotted against the peak electron density $\hat{n}_e$. At high density the variation of τ_{Eo} is akin to the neoclassical, indicating that the core of the plasma may be dominated by neoclassical losses.

Fig.11 The peak ion temperature and profile deduced by attributing the entire heat flux to neoclassical ion conduction loss, at $\bar{n}_e = 5.5 \times 10^{14} cm^{-3}$. The deduced peak ion temperature agrees with measured $\hat{T}_i = 605 eV$. An anomaly factor δ is included. At this density, an anomaly in ion thermal conduction, if any, is less than 1.5 of neoclassical. D_2 plasma, $B_T = 6T$, $I_p = 130 kA$.

Fig.12 Ion temperature much higher than electron temperature is deduced, in contradiction with experiment, when the loss of all plasma energy is attributed to neoclassical ion thermal conduction at low density, $\bar{n}_e = 1.4 \times 10^{14} cm^{-3}$. D_2 plasma, $B_T = 6T$, $I_p = 143 kA$.

Fig.13 Ratio of the measured electron heat flux to the corresponding neoclassical electron heat flux for low and high density discharges.

Fig.14 Variation with density of the experimental thermal diffusivity for electrons, χ_e^{EX} (solid circles) and ions χ_i^{EX} (open circles). $\chi_e^{EX} \propto 1/\bar{n}_e$. For comparison, the corresponding neoclassical thermal diffusivities, χ_i^{NC} and χ_e^{NC}, for ions and electrons respectively, are also shown.

Fig.15 Radial profiles of electron temperature and density for deuterium plasmas at $\bar{n}_e \simeq 2 \times 10^{14} cm^{-3}$, $I_p \simeq 115 kA$, with $B_T = 3.5T$ and 7.7T.

Fig.16 Variation of $\tau_E(EX)$ with B_T.

Fig.17 Energy confinement time in high current discharges (solid points), compared to the corresponding neoclassical values, $\tau_E(NC)$, and to the energy confinement time at low current. D plasmas, $B_T = 6T$, $215 kA \leqslant I_p \leqslant 235 kA$.

Fig.18 Variation of the quality factor, $\hat{n}\tau_E$, with density, showing $\hat{n}\tau_E \propto \bar{n}_e^2$.

V_L (1.6 V/div)

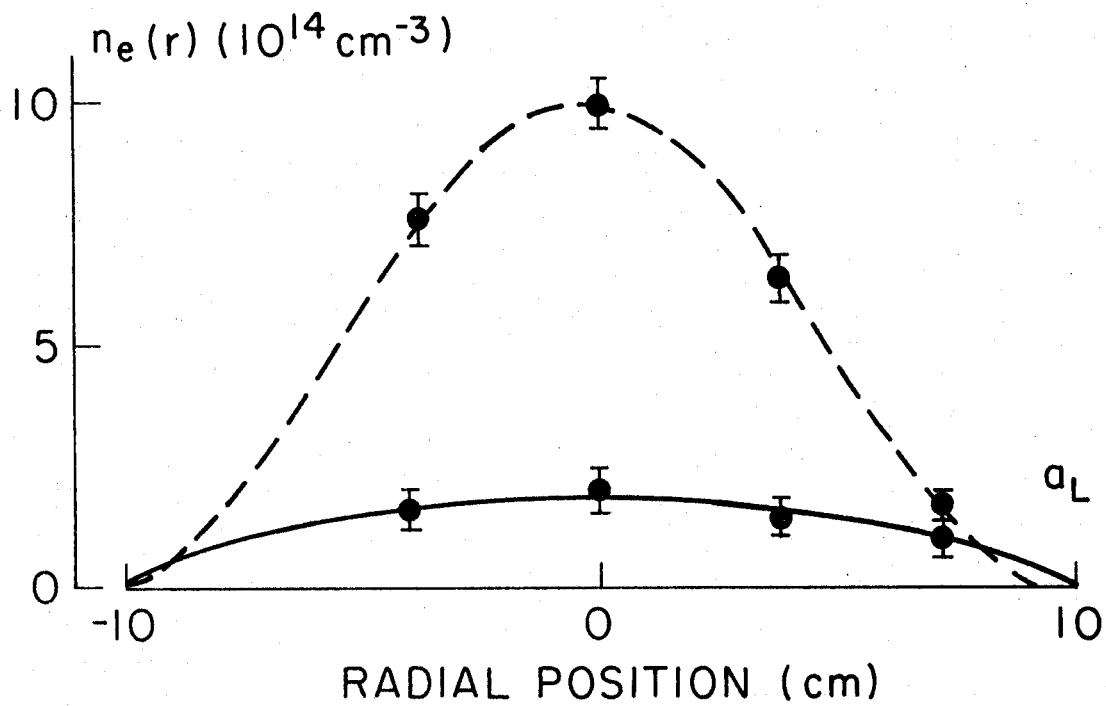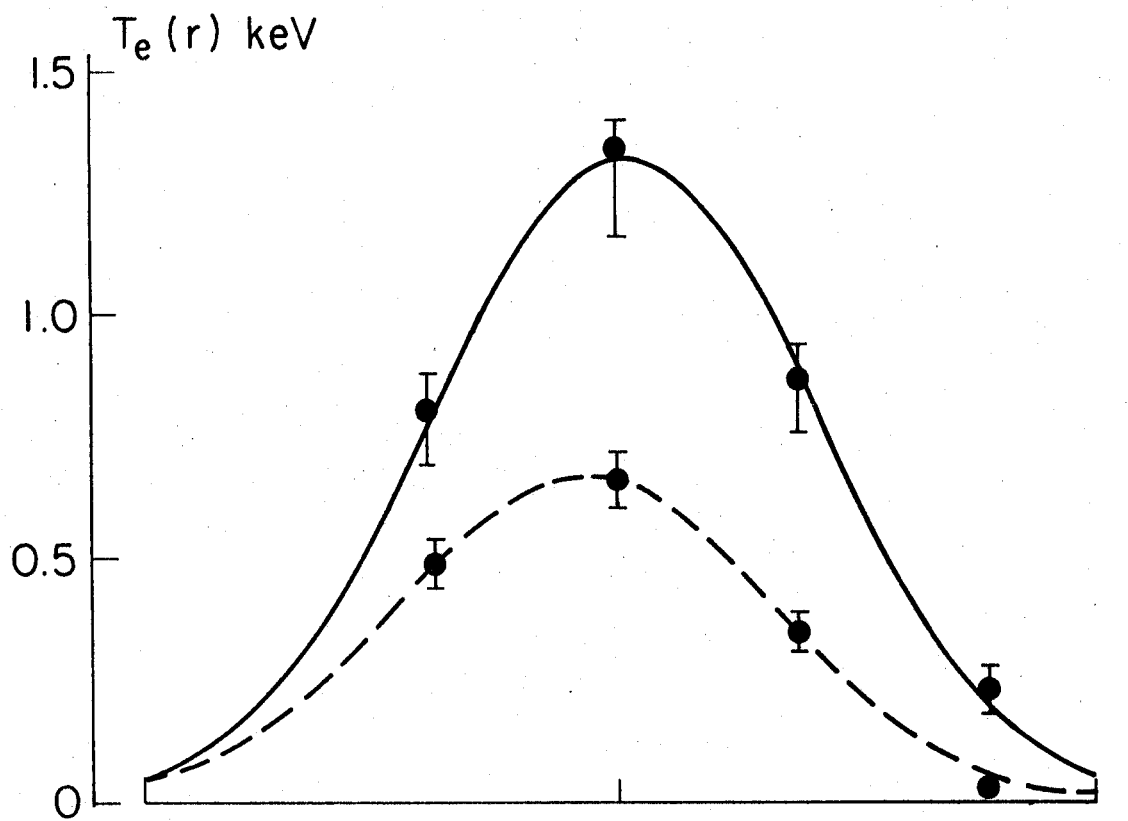I_p (50 kA/div)
$\bar{n}_e$ (10^{14} cm^{-3}/fr)
POSITION
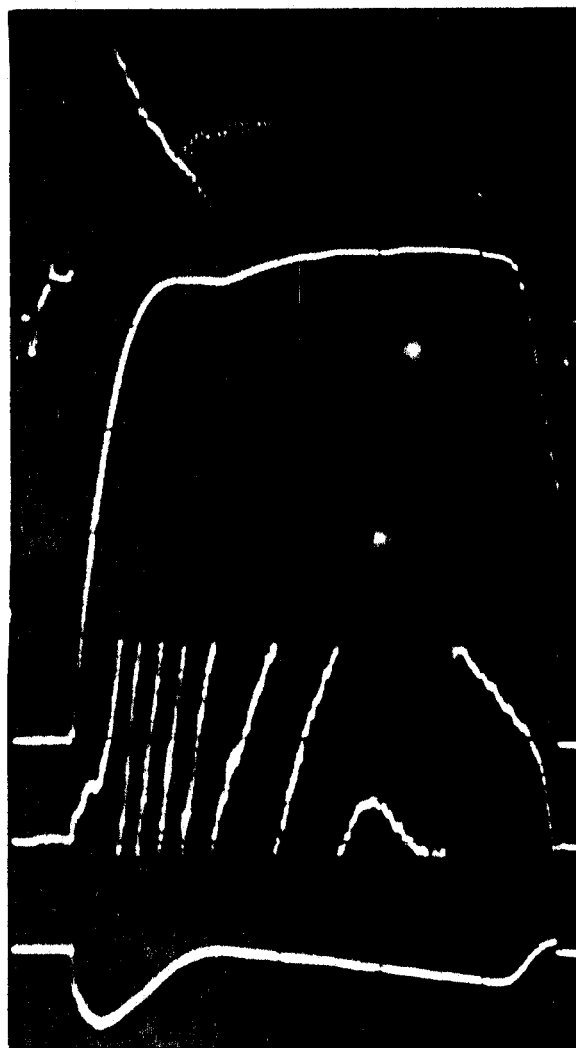
D_2 B_T = 8·7 T

Fig. 1

Fig. 2

$\bar{n}_e = 1.4 \times 10^{14} \, \text{cm}^{-3}$

$\langle \xi \rangle = 0.019$

$\langle E/E_{CR} \rangle = 0.027$

$\bar{n}_e = 5.5 \times 10^{14} \, \text{cm}^{-3}$

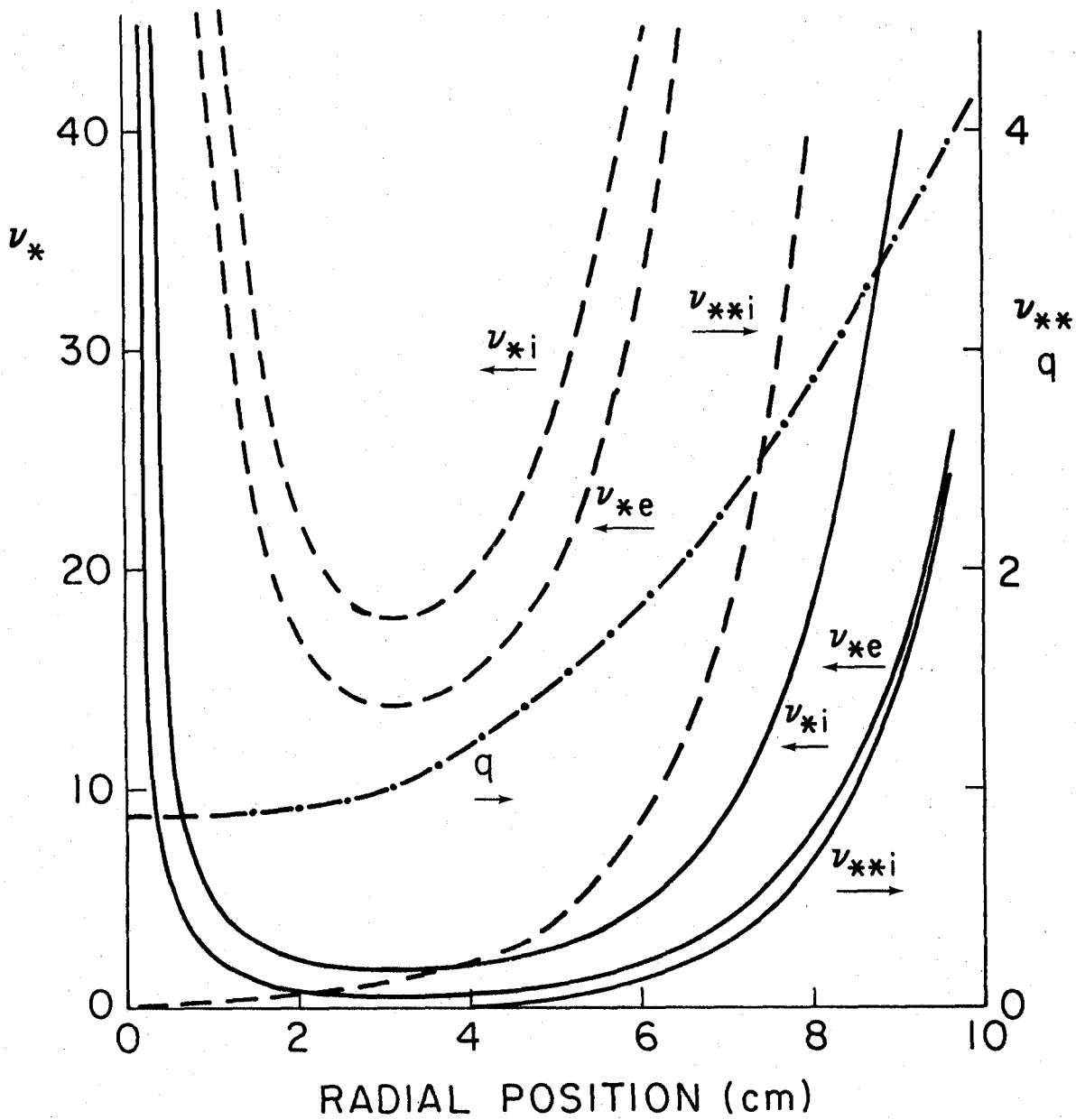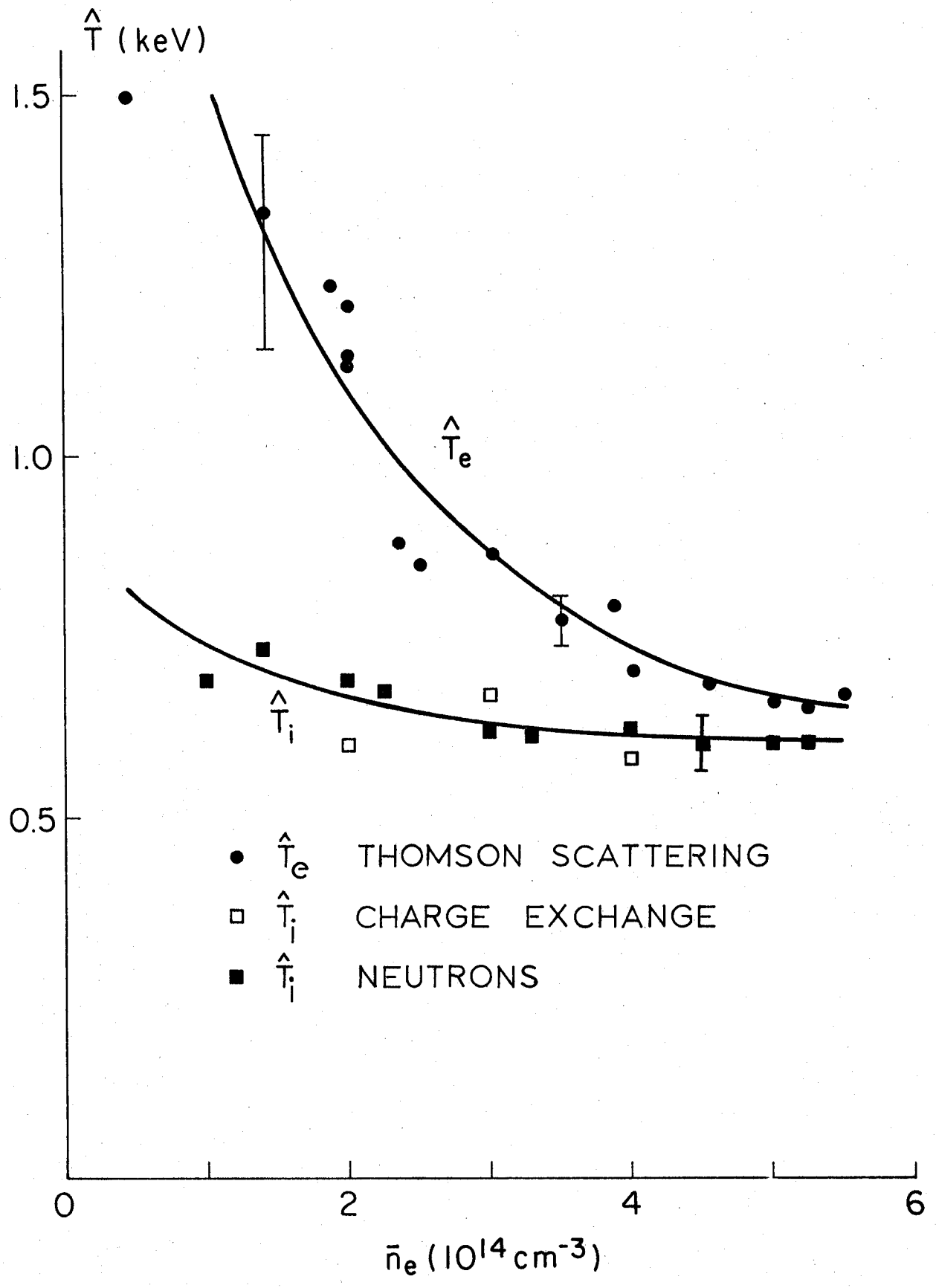$\langle \xi \rangle = 0.005$

$\langle E/E_{CR} \rangle = 0.005$

ν_*

40

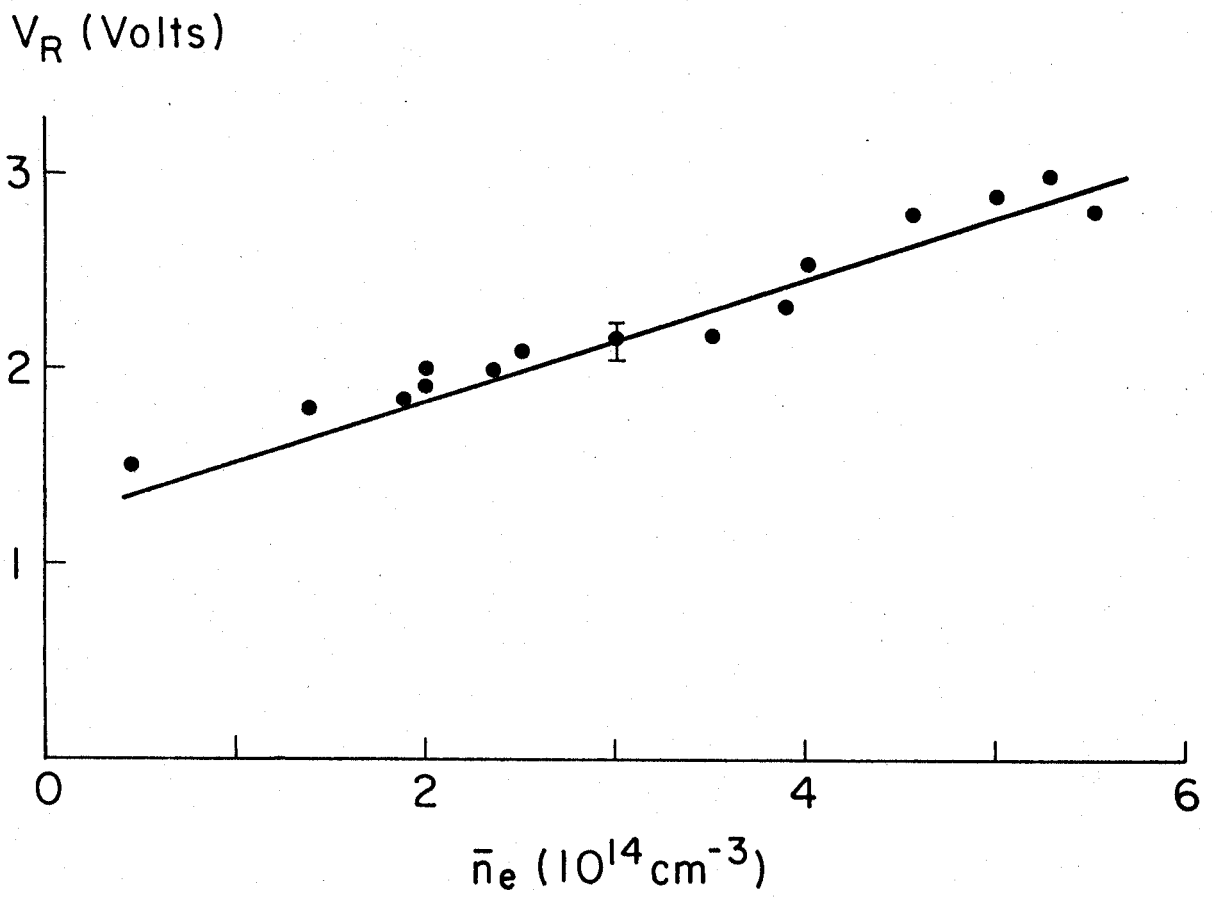30

20

10

0

ν_{*i}

ν_{**i}

ν_{*e}

ν_{*e}

ν_{*i}

ν_{**i}

q

ν_{**}

q

4

2

0

0   2   4   6   8   10

RADIAL POSITION (cm)

Fig. 3

Fig. 4

Fig. 5

$$\tau_E(NC) = \left\langle \frac{\int_0^r 2\pi r' \left\{ \frac{3}{2}(n_i T_i + n_e T_e) \right\} dr'}{2\pi r \, Q_i^{NC}(r)} \right\rangle$$

$$\tau_E(EX) = \frac{4\pi^2 R \int_0^{a_L} \frac{3}{2}(n_i T_i + n_e T_e) \cdot r dr}{V_R \cdot I_P}$$

Fig. 6

$$\beta_P = \frac{8\pi \langle n_i T_i + n_e T_e \rangle}{B_P^2}$$

Fig. 7

Fig. 8

$$\langle \nu_{*e} \rangle = \left\langle \frac{\sqrt{2}\, \nu_{ei}\, Rq}{V_{the}} \left(\frac{R}{r}\right)^{3/2} \right\rangle$$

Fig. 9

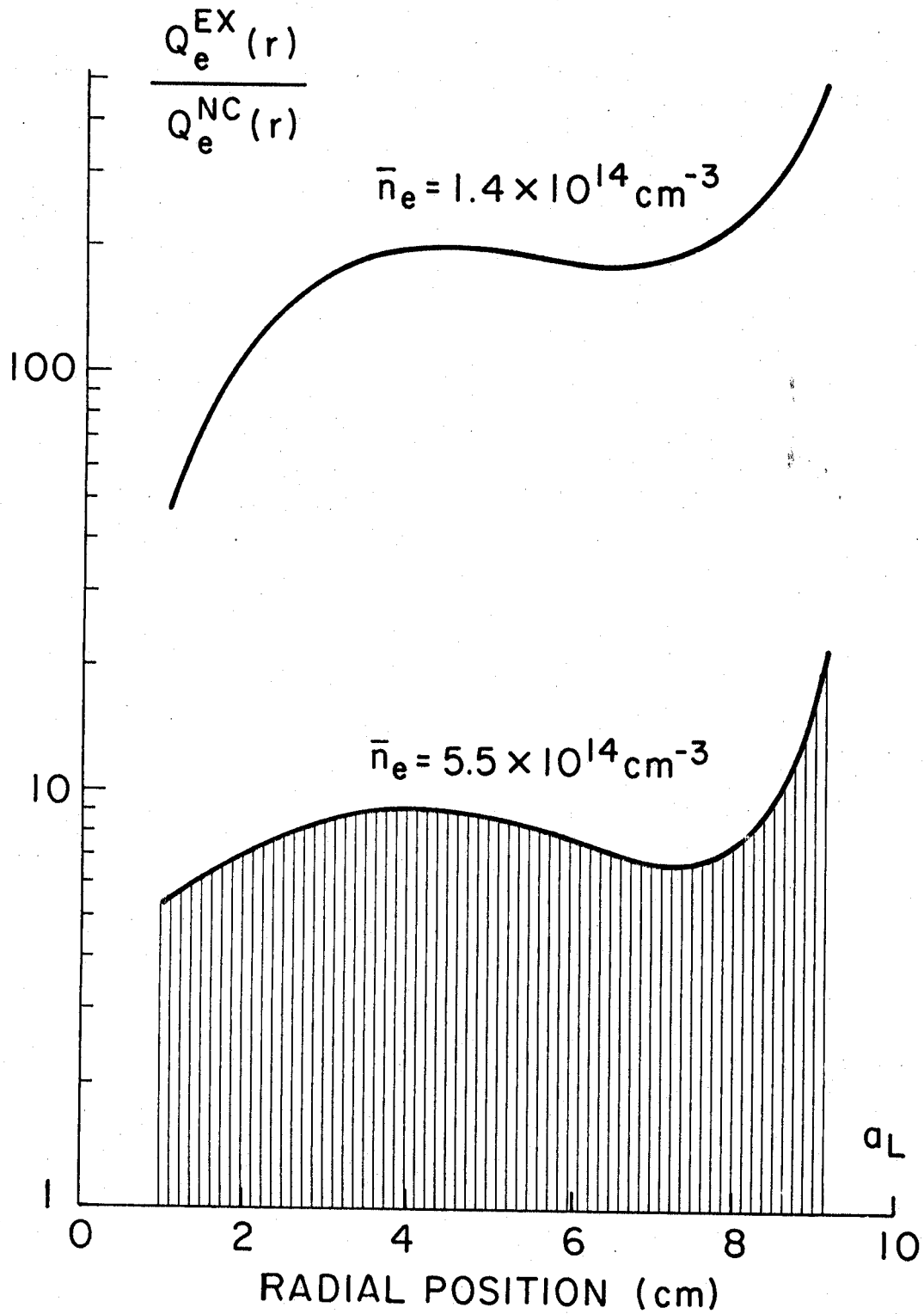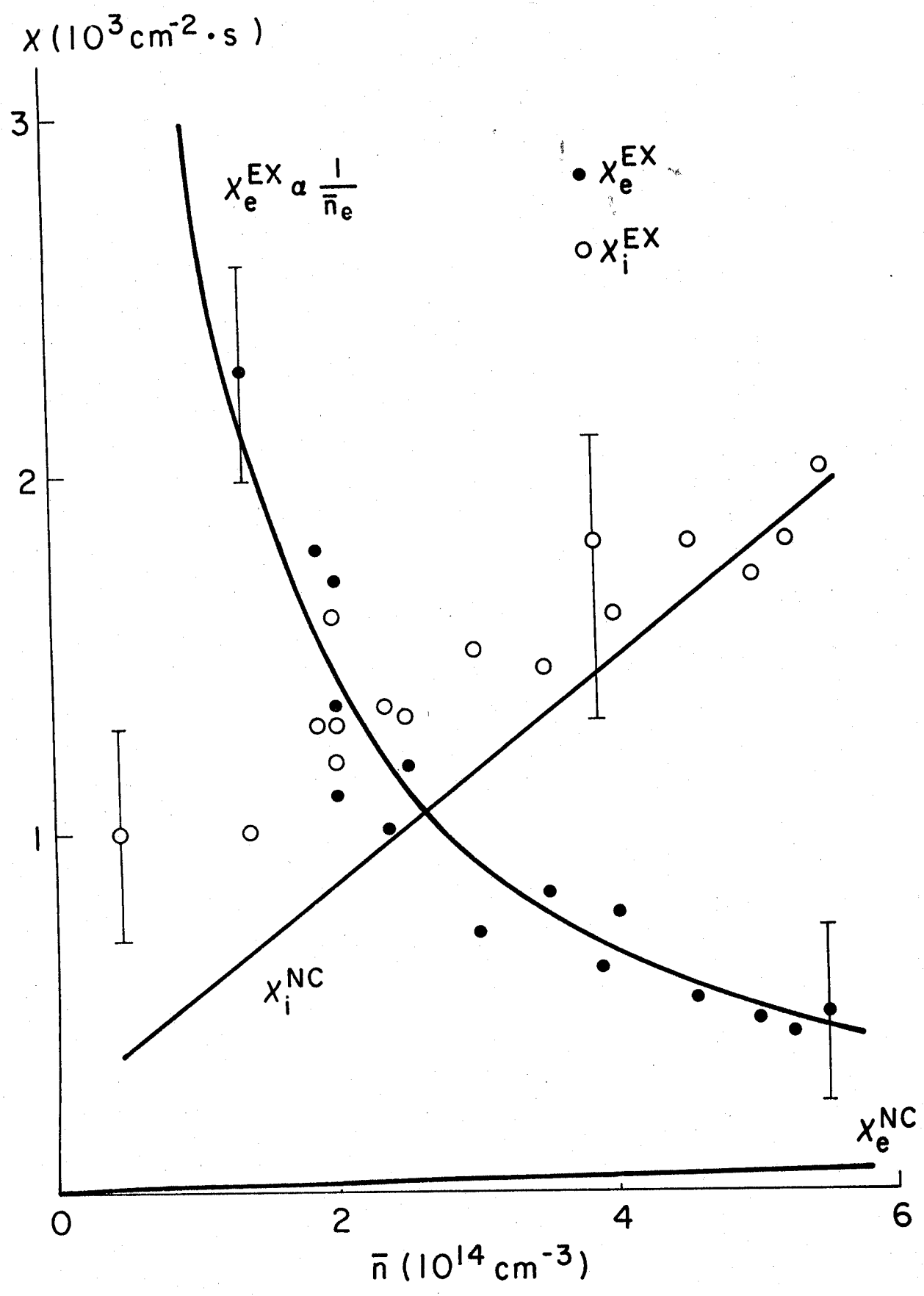$$\tau_{EO} = \frac{\frac{3}{2}(\hat{n}_i \hat{T}_i + \hat{n}_e \hat{T}_e)}{E \cdot j_0}$$
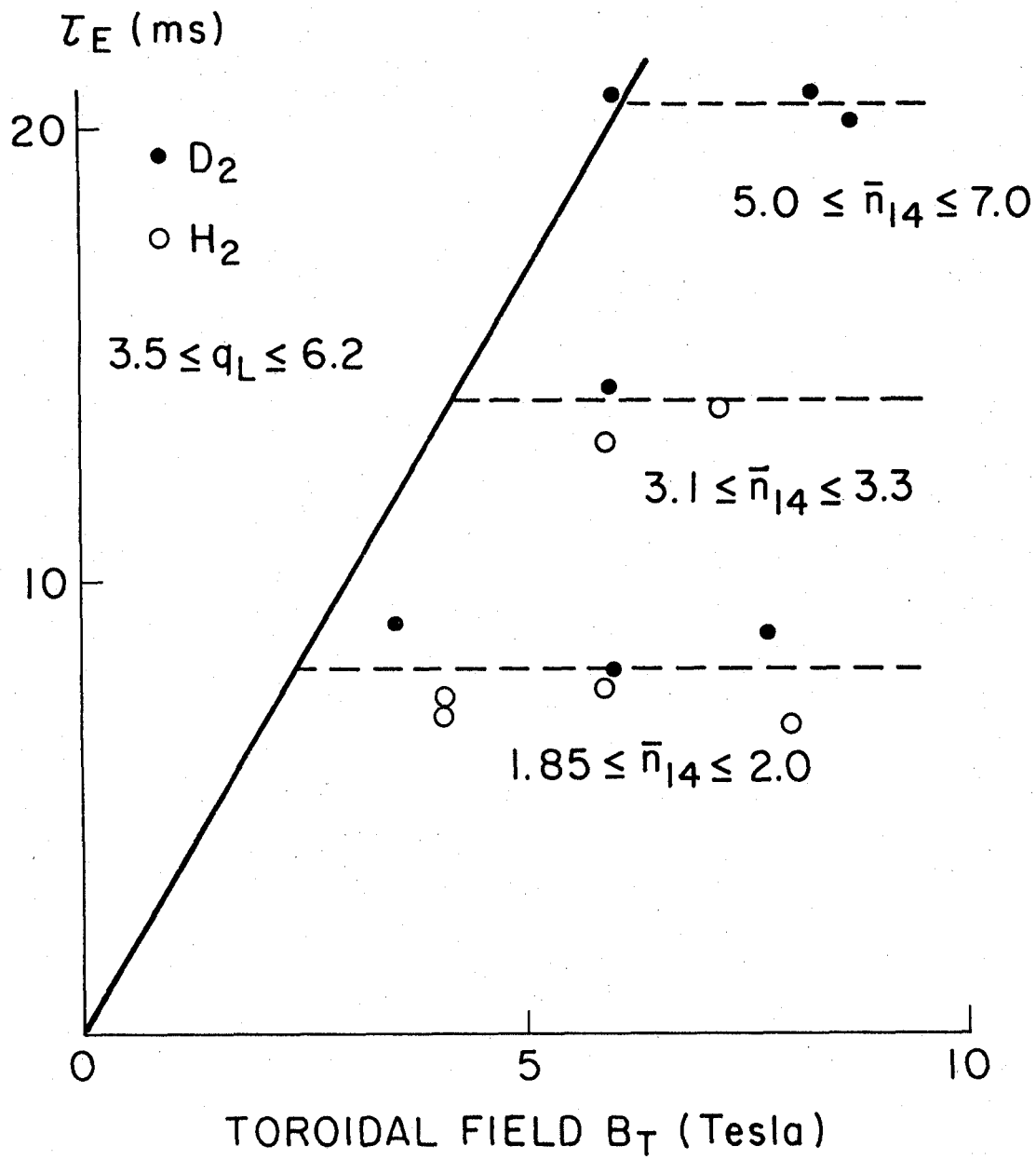
Fig. 10

Fig. 11
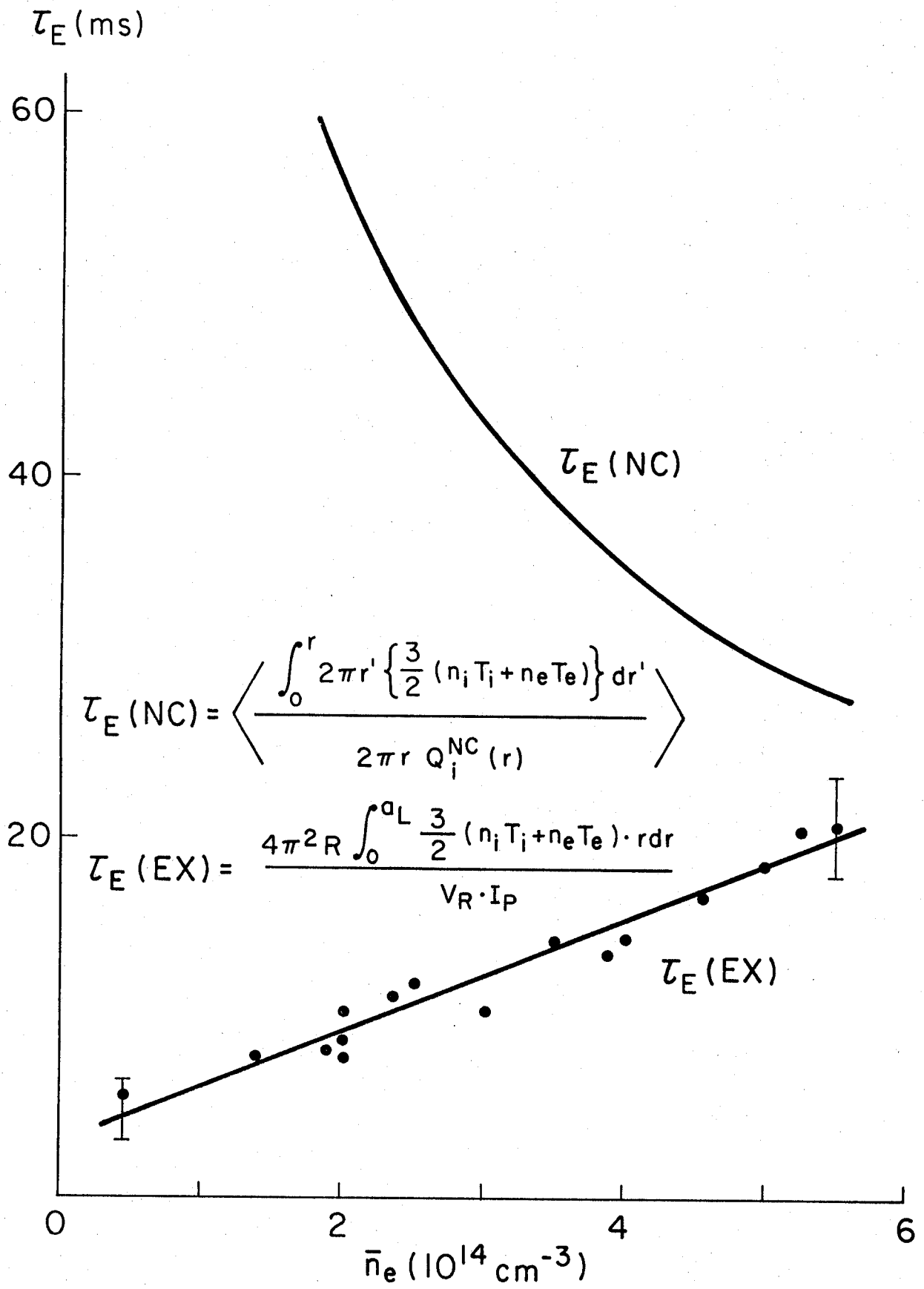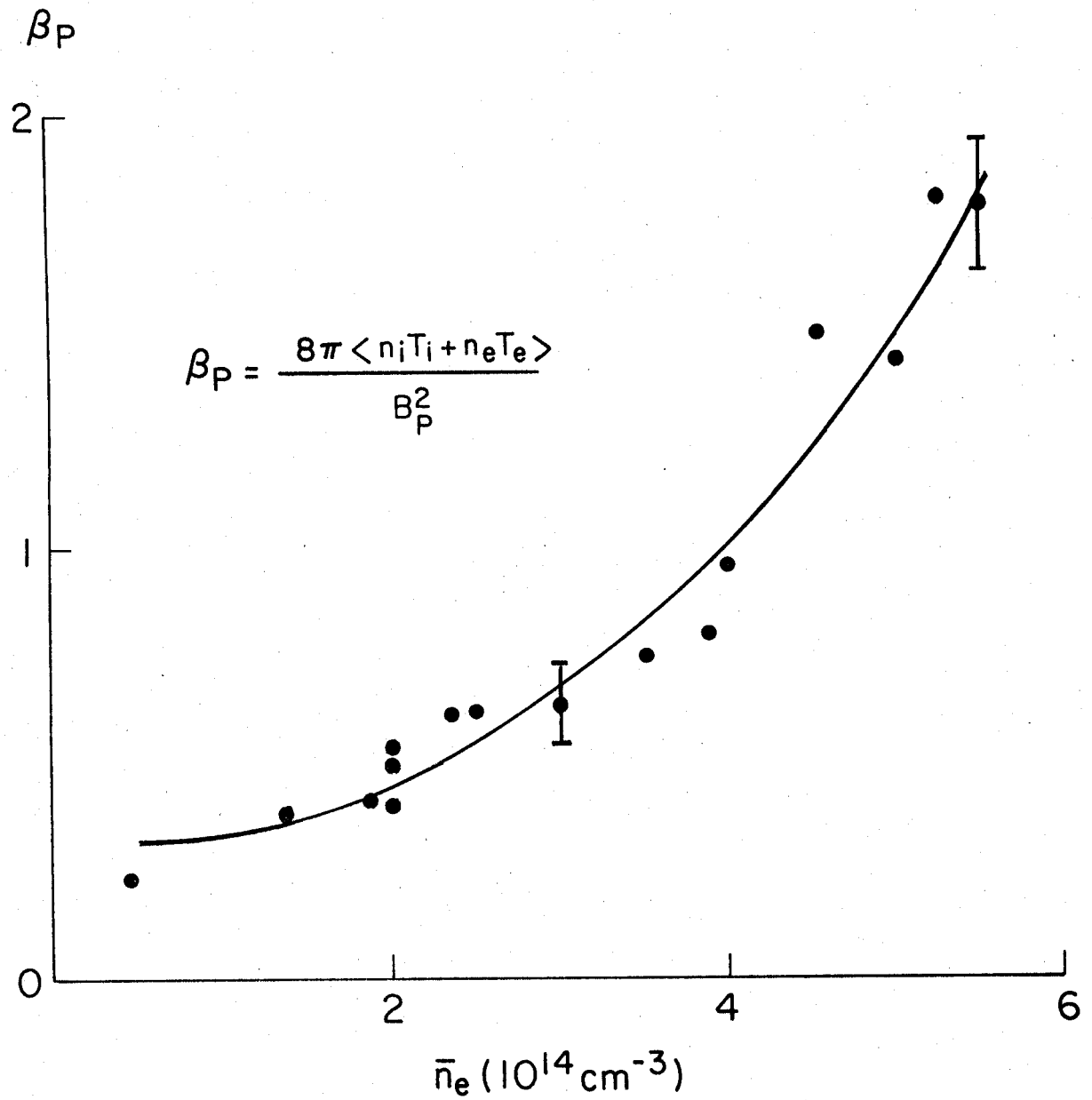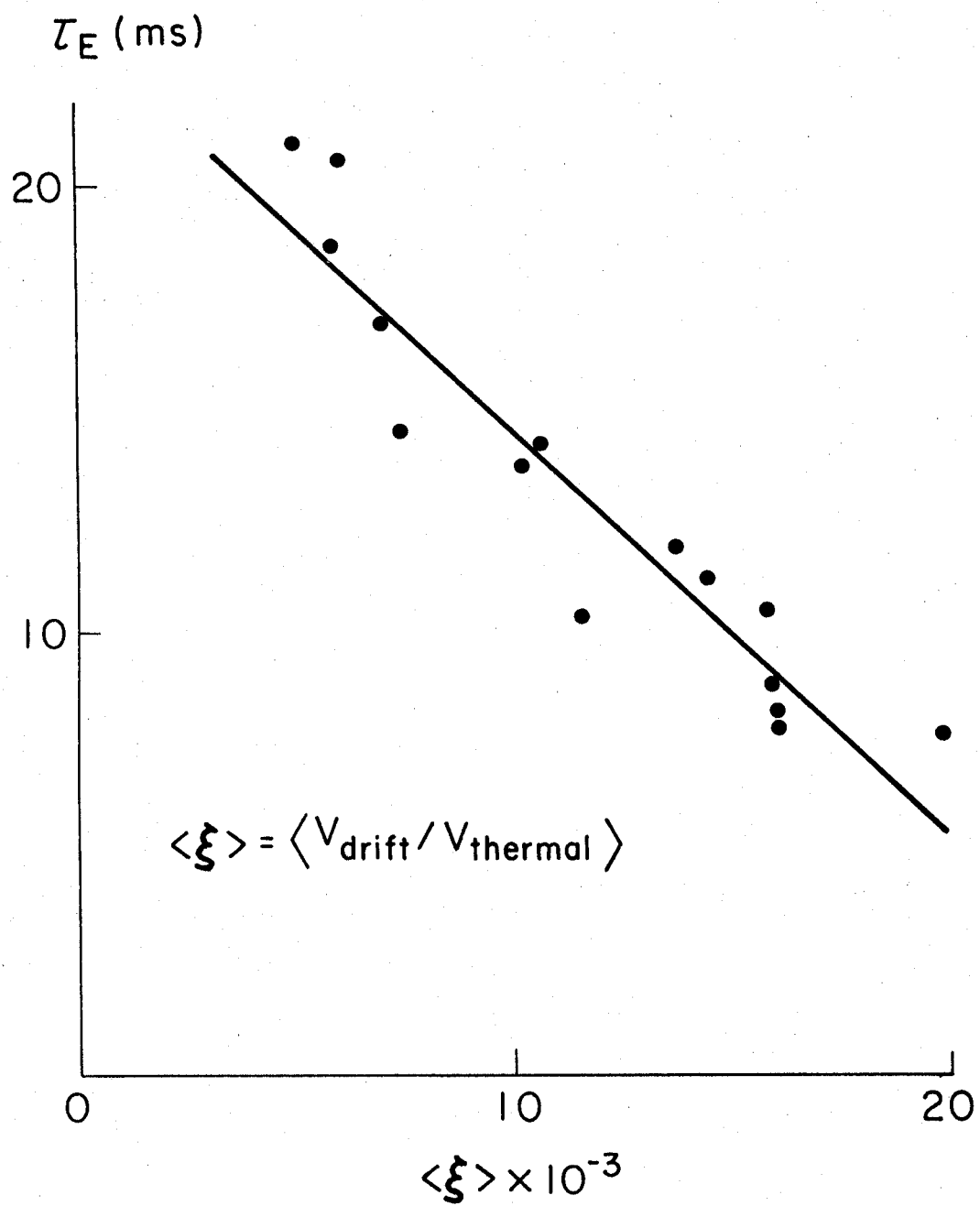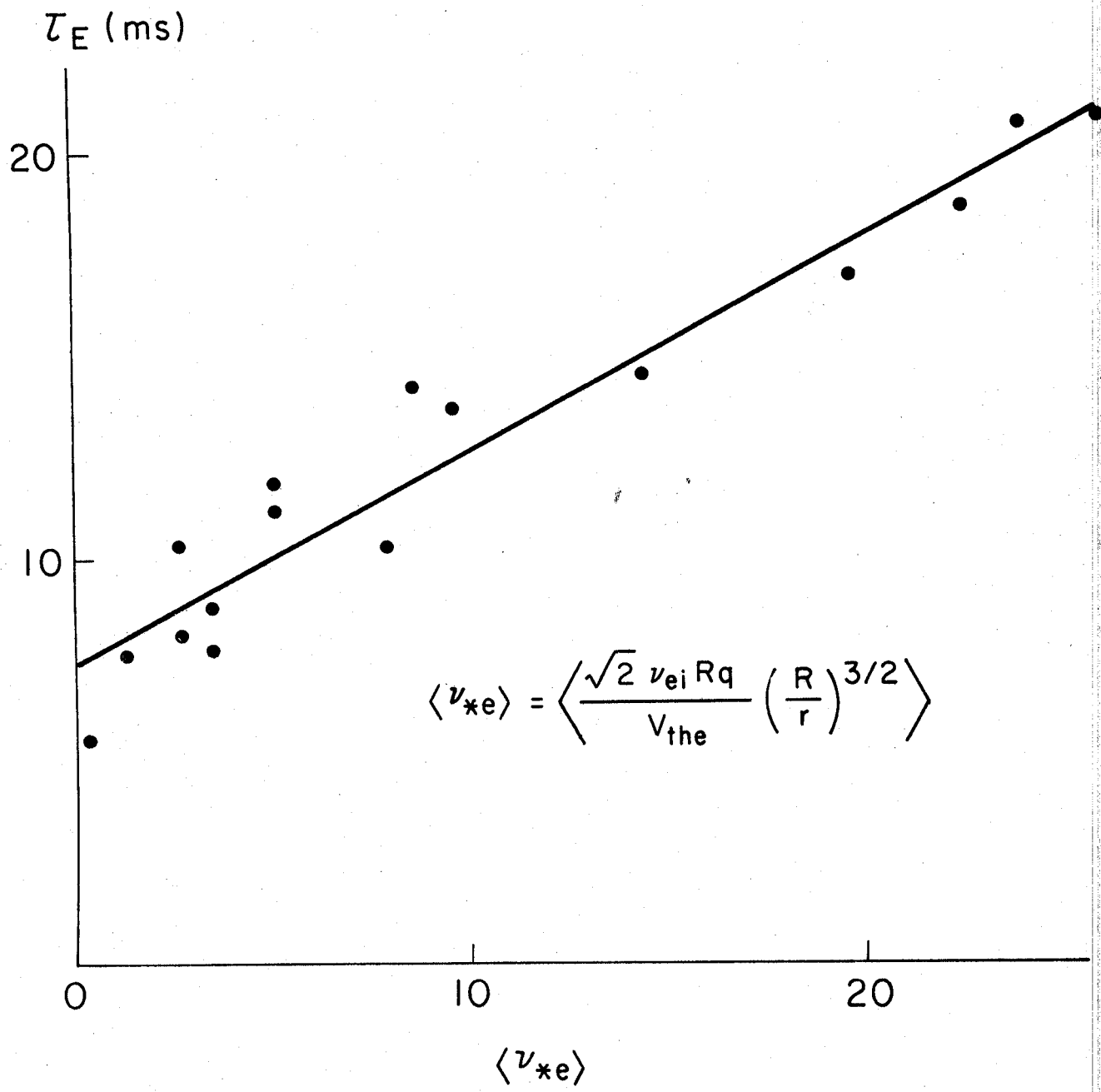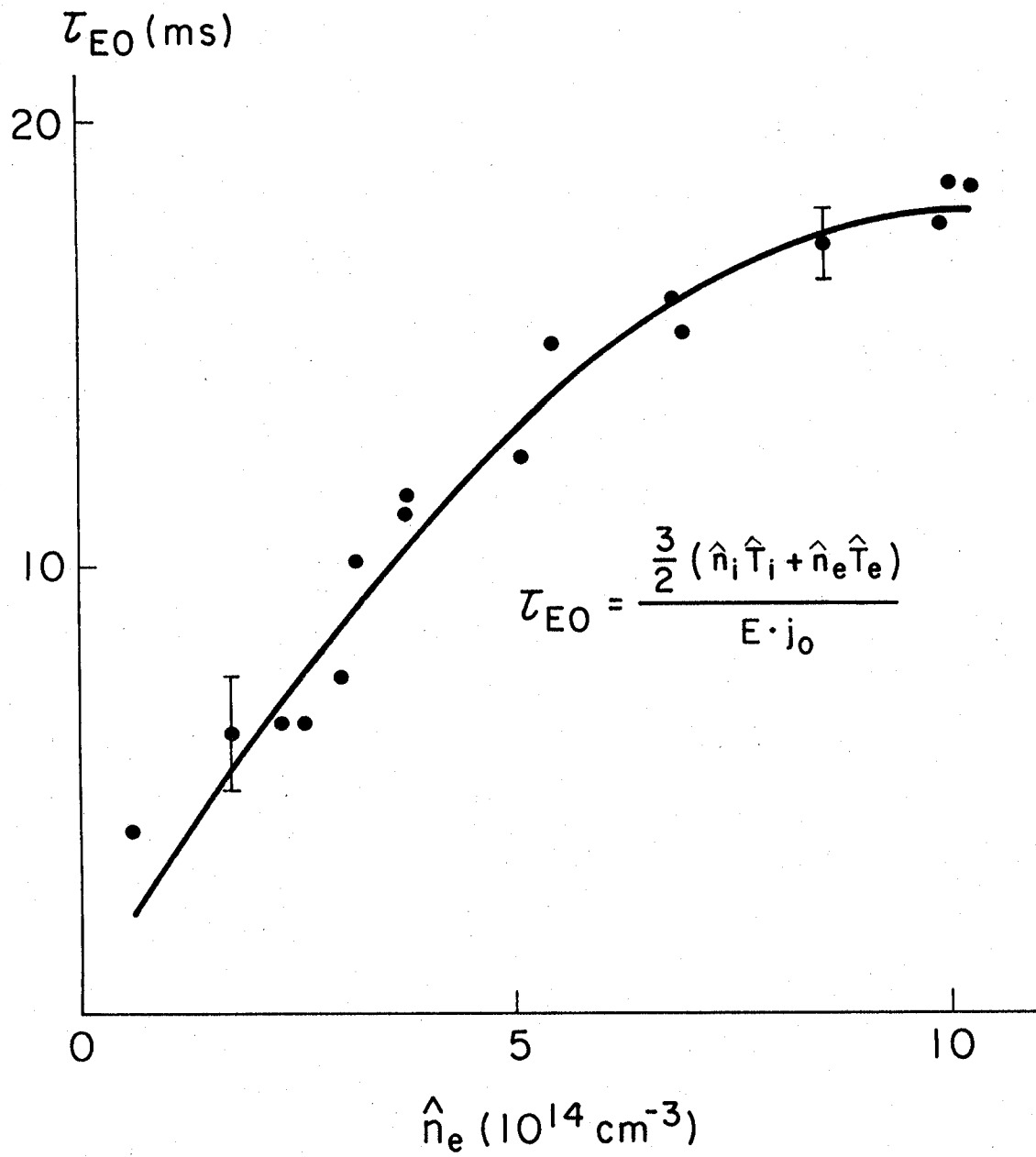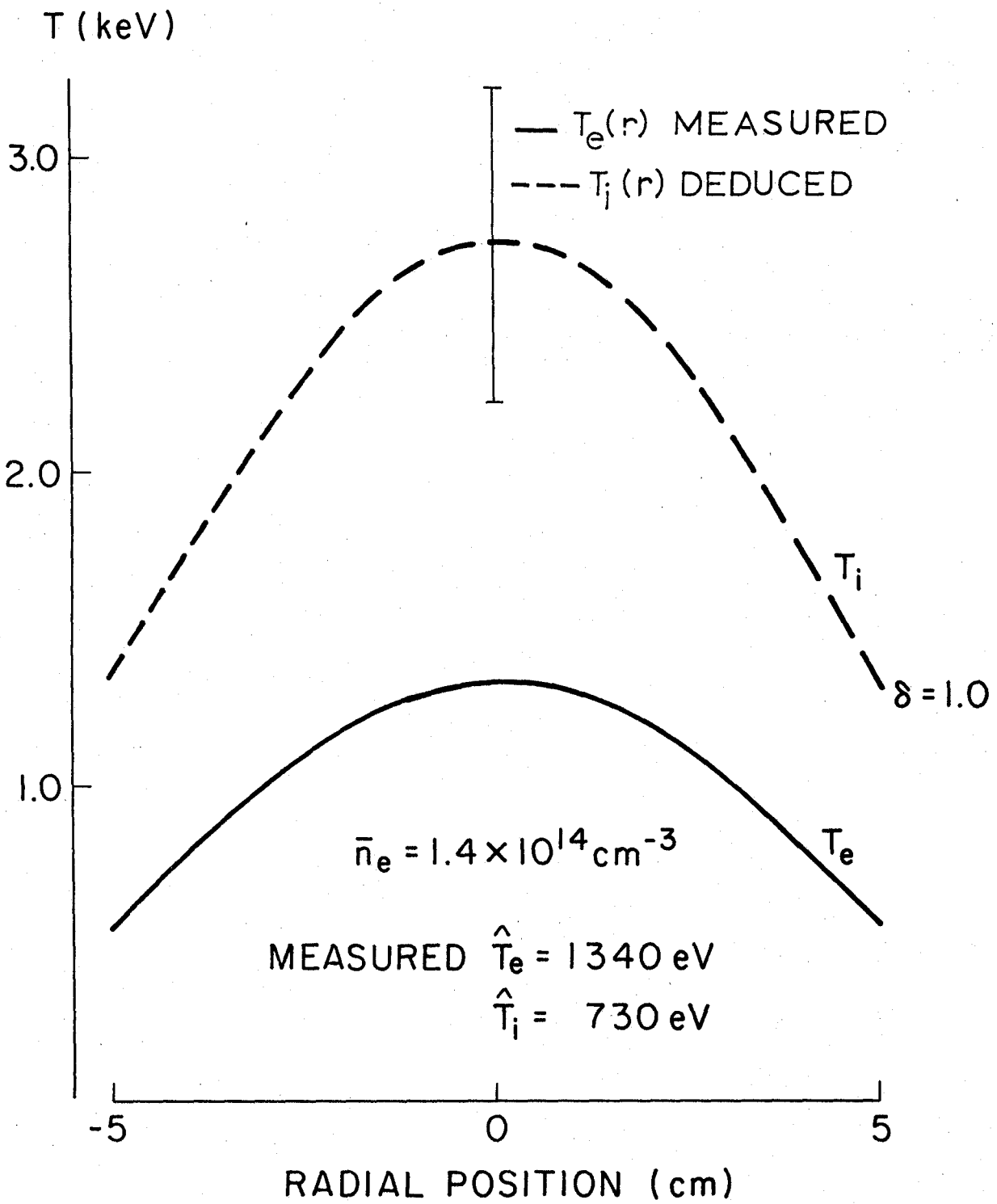
Fig. 12

Fig. 13

Fig. 14

Fig. 15

Fig. 16
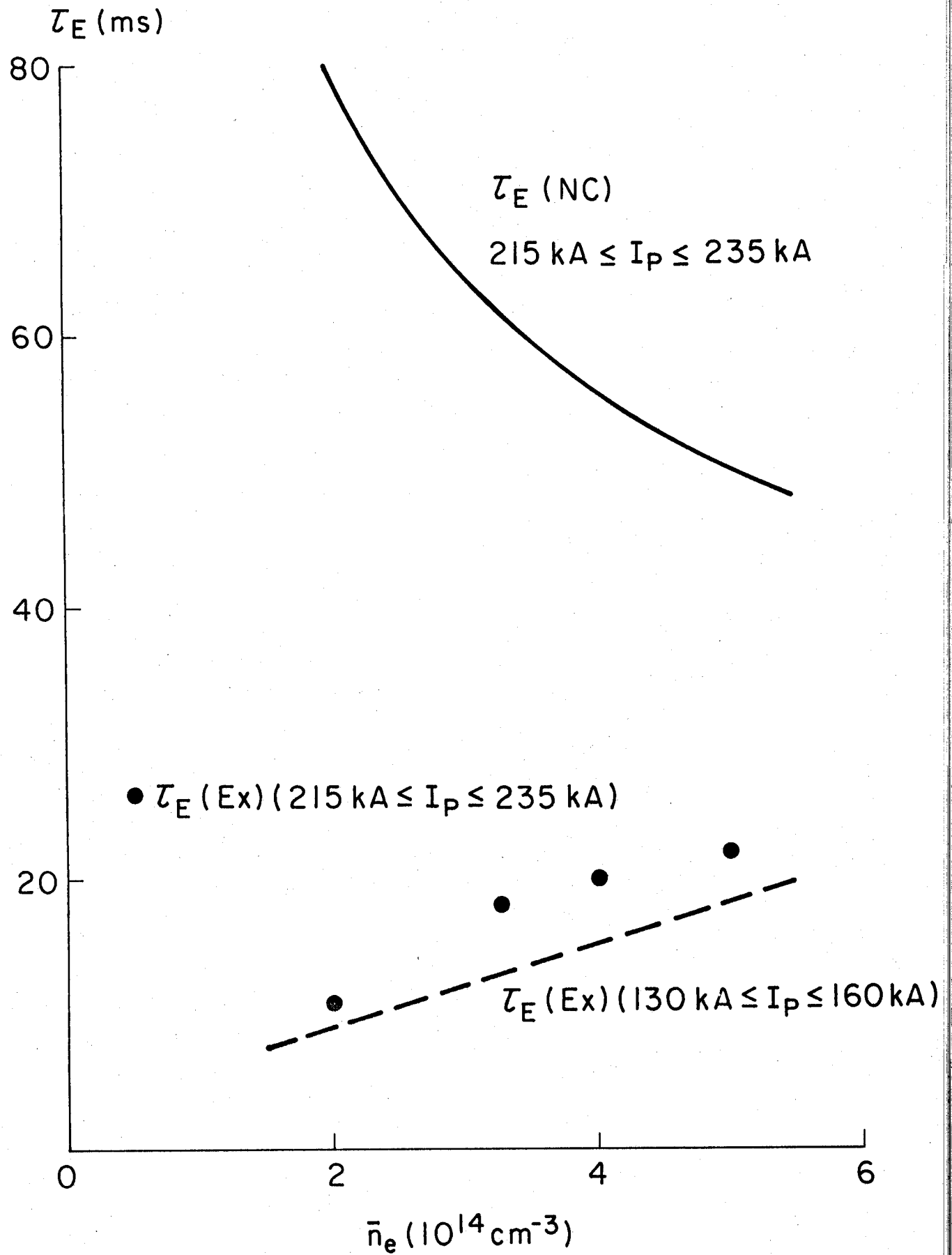
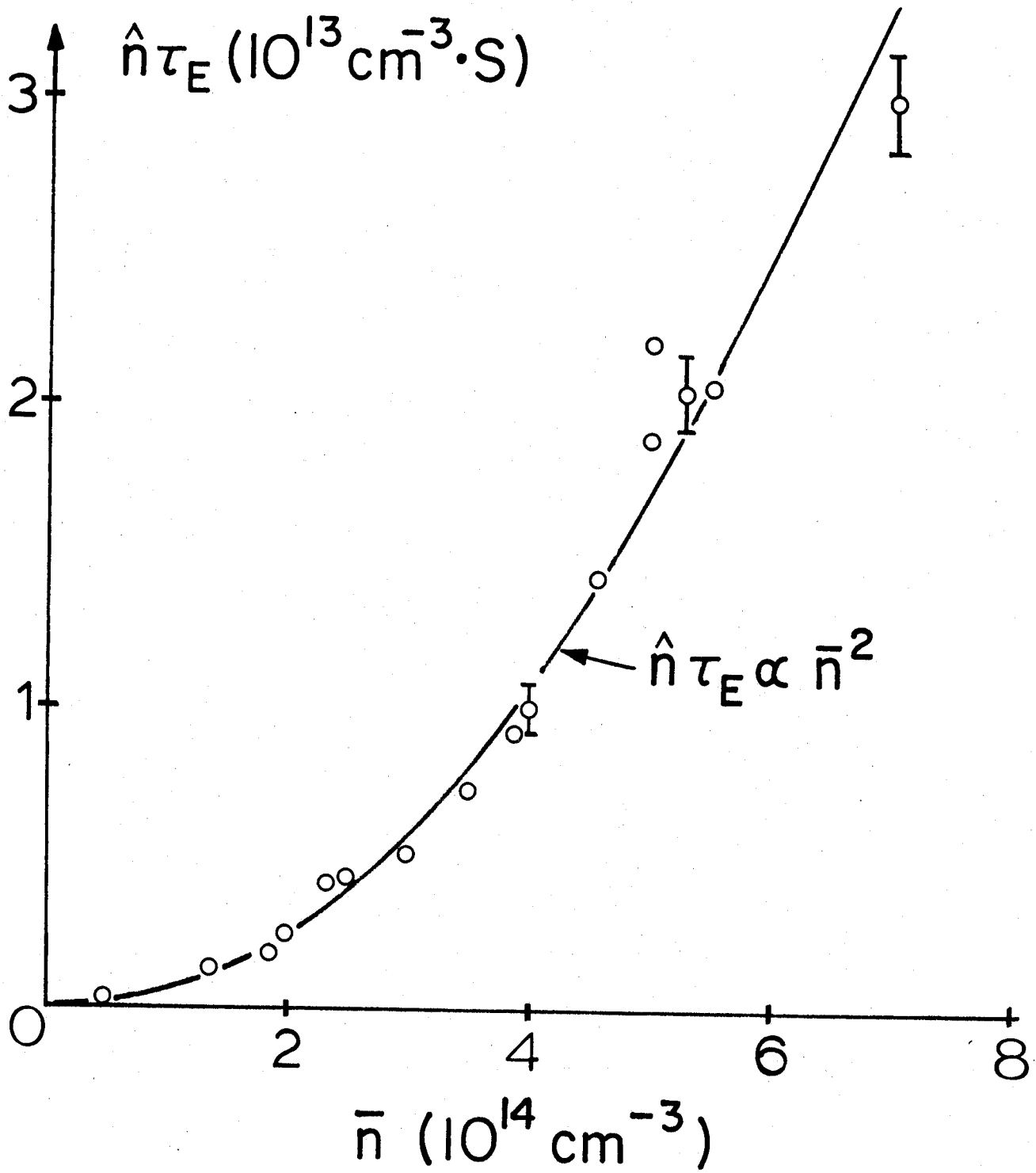τ_E (ms)

τ_E (NC)

$215\,\text{kA} \leq I_P \leq 235\,\text{kA}$

● τ_E (Ex) $(215\,\text{kA} \leq I_P \leq 235\,\text{kA})$

τ_E (Ex) $(130\,\text{kA} \leq I_P \leq 160\,\text{kA})$

$\bar{n}_e$ $(10^{14}\,\text{cm}^{-3})$

Fig. 17

Fig. 18